Estuarine, Coastal and Shelf Science 133 (2013) 206–216

Contents lists available at ScienceDirect

Estuarine, Coastal and Shelf Science

journal homepage: www.elsevier.com/locate/ecss

Positive trends between salinity and chromophoric and fluorescent dissolved organic matter in a seasonally inverse estuary

Teresa S. Catalá [a, *], Natalie Mladenov [b], Fidel Echevarría [c], Isabel Reche [a]

[a] Departamento de Ecología and Instituto Universitario del Agua, Universidad de Granada, 18071 Granada, Spain
[b] Department of Civil Engineering, Kansas State University, Manhattan, KS, USA
[c] Departamento de Biología, Facultad de Ciencias del Mar, Universidad de Cádiz, 11510 Cádiz, Spain

ARTICLE INFO

Article history:
Received 5 April 2013
Accepted 26 August 2013
Available online 4 September 2013

Keywords:
chromophoric dissolved organic matter (CDOM)
excitation–emission matrixes (EEMs)
inverse estuary
salinity
runoff and marshes

ABSTRACT

Estuaries present high content of chromophoric and fluorescent dissolved organic matter (CDOM, FDOM) affecting the attenuation of ultraviolet and blue radiation. In temperate and tropical estuaries, the main CDOM source is riverine input that generally mixes conservatively with the oceanic waters leading to negative relationships between CDOM and salinity. In Mediterranean estuaries, riverine inputs are more limited or absent during the dry season producing a negative hydrological budget and, consequently, hypersalinity and an inverse circulation pattern. Much remains to be understood about CDOM and FDOM dynamics during rainy and dry periods in these last estuaries. In this study, we determined DOM absorbance and fluorescence in the Bay of Cádiz, Spain during a rainy (high riverine inputs) and dry (hypersaline conditions) period. We determined the absorption coefficients at 355 nm (a_{355}) and acquired excitation–emission matrices (EEMs). The EEMs showed two fluorescence peaks associated with terrestrial humic-like components (peaks A and C), one peak considered to be a marine humic-like component (peak M), and two peaks considered to be amino acid-like components (peaks T and B). The a_{355} values ranged from 0.30 to 1.99 m^{-1} with the highest values during the dry season. From the rainy season to the dry season, the overall fluorescence intensity increased and fluorescent peaks M, B, and T increased by greater than two orders of magnitude, whereas the fluorescence intensities of peaks A and C changed less than one order of magnitude. Unlike temperate and tropical estuaries, the a_{355} values and fluorescence of the five peaks were positive and significantly related to salinity, but with different slopes. The inverse nature of the Bay of Cádiz during the dry season could be responsible for these positive trends between CDOM/FDOM and salinity. The slopes of the humic-like peaks A and C were lower than the a_{355} slope suggesting their preferential losses, likely due to photobleaching. By contrast, the slopes of the amino acid-like peaks B and T were higher than the a_{355} slope suggesting an *in situ* production of these fluorophores, likely due to diffusion from salt marsh and coastal sediments.

1. Introduction

In marine systems, chromophoric or colored dissolved organic matter (CDOM) absorbs ultraviolet radiation and is largely responsible for its attenuation (Coble, 2007; Nelson and Siegel, 2013). A portion of CDOM also emits fluorescence when irradiated with ultraviolet light and is termed fluorescent dissolved organic matter (FDOM) (Coble, 1996, 2007). CDOM absorption can even extend into the blue wavelength band, thereby diminishing the potential for primary productivity (overlapping one of the chlorophyll *a* absorption peaks) and influencing ocean color algorithms for remote sensing (Bowers et al., 2004; Siegel et al., 2005; Granskog et al., 2007; Ortega-Retuerta et al., 2010a; Nelson and Siegel, 2013).

Optical spectroscopy of dissolved organic matter (DOM) provides information on DOM origin, average size, diagenetic status (fresh vs. aged) and degradability (Stedmon et al., 2003; Stedmon and Markager, 2005; Coble, 2007; Helms et al., 2008; Fellman et al., 2008; Guo et al., 2011). The use of fluorescence spectroscopy allows for the identification of amino acid-like fluorophores (peaks B and T after Coble (1996)), which have been shown to represent biodegradable and fresh DOM (Yamashita and Tanoue, 2003; Fellman et al., 2008). In contrast, humic-like fluorophores (peaks A, C and M after Coble (1996)) appear to be photodegradable, but biorefractory (Maie et al., 2012). In the open ocean, the main origin of DOM is autochthonous, and this DOM comprises more than 95% of the total organic matter pool (Lalli and Parsons,

* Corresponding author.
E-mail address: teresc@ugr.es (T.S. Catalá).

0272-7714/$ – see front matter © 2013 Elsevier Ltd. All rights reserved.
http://dx.doi.org/10.1016/j.ecss.2013.08.030

1997; Nelson and Siegel, 2013), whereas terrestrial inputs only represent about 2–3% of the total DOM. Nevertheless, these terrestrial inputs can be more relevant in coastal zones (Opsahl and Benner, 1997), where they may represent between 20% and 70% of the DOM pool (Del Castillo et al., 1999). In coastal and estuarine systems, the origin of humic-like fluorophores was considered to be mostly from fluvial discharge (Coble et al., 1998; Gardner et al., 2005). Now we know that autochthonous sources, such as phytoplankton (Romera-Castillo et al., 2010), bacteria (Nelson et al., 2004; Ortega-Retuerta et al., 2009; Romera Castillo et al., 2011), zooplankton (Steinberg et al., 2004), seagrasses (Stabenau et al., 2004; Barrón and Duarte, 2009) and sediments (Burdige et al., 2004; Tremblay et al., 2007) also contribute chromophoric, humic like components. In addition, at the terrestrial–marine interface, salt marshes are a continuous source of CDOM linked to the tidal cycle (Clark et al., 2008; Tzortziou et al., 2008; Bianchi et al., 2010).

Temperate and tropical estuarine and coastal systems with continuous riverine inputs undergo conservative mixing between the fluvial inputs and oceanic waters. This conservative mixing has been widely reported in the literature and characterized by negative linear relationships between salinity and CDOM and FDOM (e.g. Del Castillo et al., 1999; Jaffé et al., 2004; Kowalczuk et al., 2006; Guo et al., 2007; Bowers and Brett, 2008; Osburn and Stedmon, 2011). Among all the fluorescent DOM components, terrestrial humic-like components consistently have negative trends with salinity under conservative mixing conditions, whereas amino acid-like components do not (Kowalczuk et al., 2005; Yamashita et al., 2008; Osburn and Stedmon, 2011).

In Mediterranean regions with long and dry summers, estuaries and bays receive low or no fluvial discharge, and evaporation can exceed the freshwater supply, producing hypersalinity in the estuary compared to adjacent oceanic waters (Corlis et al., 2003; Nunes-Vaz, 2012). This seasonal process alters estuarine circulation patterns from classical (fluvial waters spread seaward over the inflowing more dense oceanic waters) to inverse (hypersaline waters drain out below less dense oceanic waters) and represents a major class of estuaries typical of the Mediterranean climate (Largier et al., 1997). During the dry season in inverse estuaries, CDOM derived from marshlands flushed by the tidal cycle (Clark et al., 2008), sediments (Burdige et al., 2004; Tremblay et al., 2007), seagrasses (Stabenau et al., 2004; Barrón and Duarte, 2009) and anthropogenic activities (Fellman et al., 2011) may represent additional CDOM sources. To the best of our knowledge, there are no studies systematically analyzing the relationships between salinity and CDOM and FDOM in inverse estuaries, although Milbrandt et al. (2010) have reported a positive linear relationship between FDOM and salinity in the west Florida shelf for salinities greater than 36.5 psu.

In this study, we described the CDOM optical properties (absorption and fluorescence) in a seasonally inverse estuary, the Bay of Cádiz. Two contrasting seasons were studied: spring with intense rainfall and fluvial discharge and summer with absence of rainfall, reduced fluvial discharge, hypersaline conditions, and inverse circulation. We evaluated the trends between salinity and CDOM in this class of estuary and assessed the alternative CDOM and FDOM sources linked to riverine discharge compared to marshes or sediments during the dry season.

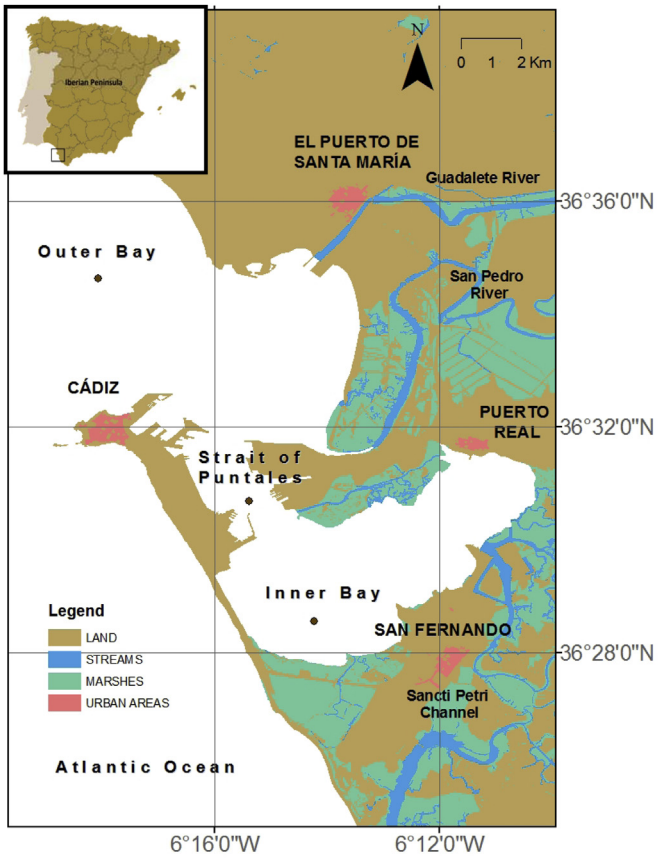

Fig. 1. Map of the Bay of Cádiz, its location in Spain (superior square) and the locations of the three sampling stations: the Inner Bay (with low influence of riverine discharges but surrounded by salt marshes), the Strait of Puntales (with influence of inputs from Guadalete River and from the Inner Bay during ebb tides) and the Outer Bay (the most oceanic station).

Table 1
Location, depth and physical characteristics and values for concentration of DOC, chlorophyll *a* and optical properties in the Inner Bay, Strait of Puntales and Outer Bay. a_{355} is the absorption coefficient at 355 nm, ε_{355} is the molar absorption coefficient at a_{355} (a_{355}/DOC), SR is the ratio S275–295/S350–400, FI is the fluorescence index and λ_{max} is the emission wavelength of the maximum fluorescence intensity at 370 nm.

	Date	Depth (m)	Salinity	Temperature (°C)	DOC (μM)	Chl (μg l^{-1})	a_{355} (m^{-1})	ε_{355} (m^2 mol^{-1})	S_R	FI	λ_{max} (nm)
Inner Bay	24/03/2010	Surface	34.96	16.51	221	6.37	0.52	2.33	1.20	1.49	462
	05/05/2010		36.17	19.18	148	2.59	0.84	5.70	1.48	1.58	462
	10/06/2010		36.65	22.06	139	2.66	0.73	5.24	124	1.54	462
Location:	01/07/2010		37.40	25.61	243	0.83	1.29	5.31	1.34	1.49	462
36° 28′ N, 6° 14′ W	26/07/2010		–	–	–	–	–	–	–	–	
	14/09/2010		37.11	23.25	160	3.07	1.09	6.80	1.36	1.52	458
Strait of Puntales	24/03/	Surface	35.19	17.08	132	7.72	1.08	8.23	1.20	1.49	462
	2010	7	–	–	118	2.75	0.48	4.08	1.60	1.61	444
	05/05/	Surface	35.73	19.54	126	2.36	1.30	10.33	1.01	1.53	464
	2010	7	–	–	150	4.05	0.95	6.33	1.45	1.54	464
	10/06/	Surface	36.56	21.99	93	3.04	0.83	9.01	1.63	1.51	460
	2010	6.4	–	–	97	1.67	0.73	7.55	1.54	1.55	456
Location:	01/07/	Surface	36.59	24.16	124	5.79	0.68	5.52	1.59	1.56	472
36° 30′ N, 6° 15′ W	2010	5.8	–	–	246	3.76	0.87	3.54	1.02	1.54	458
	26/07/	Surface	37.24	25.85	189	2.04	0.90	4.77	1.33	1.55	464
	2010	3	–	–	203	2.38	1.23	6.04	1.30	1.56	464
	14/09/	Surface	37.40	23.42	153	2.59	0.90	5.87	1.38	1.54	460
	2010										
		6	–	–	477	2.92	1.99	4.17	0.85	1.59	458
Outer Bay	24/03/	Surface	35.53	16.36	113	1.50	0.38	3.39	1.78	1.50	464
	2010	9	–	–	83	1.27	0.30	3.57	2.05	1.48	466
	05/05/	Surface	35.85	18.82	108	6.30	0.69	6.38	1.40	1.53	460
	2010	9	–	–	104	2.62	0.50	4.76	1.75	1.60	458
	10/06/	Surface	36.35	21.96	103	5.66	0.61	5.98	1.47	1.52	460
	2010	7.9	–	–	102	2.40	0.45	4.37	1.37	1.53	466
Location:	01/07/	Surface	36.39	22.40	134	5.58	0.57	4.27	1.57	1.54	464
36° 34′ N, 6° 16′ W	2010	9.8	–	–	97	1.63	0.35	3.67	1.52	1.62	464
	26/07/	Surface	–	–	–	–	–	–	–	–	–
	2010	–	–	–	–	–	–	–	–	–	–
	14/09/	Surface	36.60	23.48	228	6.09	0.61	2.69	1.45	1.56	464
	2010	10.4	–	–	164	2.02	0.77	4.71	1.45	1.57	462

2. Study area and methods

2.1. Study site

The Bay of Cádiz is a semi-enclosed system located in the southwest of the Iberian Peninsula at 36.50 °N, 6.30 °W with an area of approximately 30,000 ha. It is divided into 2 basins, a shallower Inner Bay (depths lower than 2 m) and a deeper Outer Bay (depths between 12 and 25 m) connected by the narrow Strait of Puntales (mean depth = 11 m) (Fig. 1). The Inner Bay is a large lagoon surrounded by a muddy tidal flat and intersected by a tidal channel net. The Strait of Puntales is affected by runoff from the Guadalete and San Pedro Rivers and salt marsh inputs (mostly during the ebbing tides from the Inner toward the Outer Bay) (Fig. 1). The Guadalete River is the main freshwater stream into the Bay, but the San Pedro River, an old and artificially blocked tributary of the Guadalete River, can also be relevant during occasional inflows resulting from rainfall and land drainage. The Bay of Cádiz is subjected to a semidiurnal tidal regime providing water renewal rates of 30% during neap tides and 75% during spring tides (Álvarez et al., 1999). The vast extensions of intertidal zones and salt marshes input nutrients and organic matter into the Bay of Cádiz thereby resulting in a very productive ecosystem (González-Gordillo and Rodriguez, 2003) that also supports aquaculture (De la Paz et al., 2008; Ferrón et al., 2009; Morris et al., 2009).

The study system has a Mediterranean climate with a sparce and irregular rainfall pattern, and is also directly influenced by rapid Atlantic fronts with a mean annual precipitation of 598 mm during the 1971 to 2000 period (http://www.aemet.es). In particular, the study year (2010) was one of the rainiest years of the last half-century, with a mean annual precipitation value of 660 mm, exceeding 10% of the normal average value in this region (www.ine.es). The highest rainfall in the Bay of Cádiz occurred in March (81.6 mm). In contrast, rainfall was almost absent from July to September, and we refer to this time interval as the dry period. One of the rainiest days of our sampling period was registered on the 9th of June (17.1 mm), the day just before one of the sampling dates. Considering that maximum precipitation was measured between February and the first fortnight of March, we expect that March and June were the months most affected by terrestrial inputs. The water level of the Guadalete River was obtained from the historical database of the Andalucia Water Agency (http://www.chguadalquivir.es/saih/).

2.2. Sampling and chemical analysis

Water sampling was performed from March to September of 2010 at three different stations (Fig. 1): Inner Bay (36° 28′ N, 6° 14′ W, a station weakly influenced by streams and mostly affected by marsh inputs), Strait of Puntales (36° 30′ N, 6° 15′ W, a station influenced by the Guadalete and San Pedro Rivers), and Outer Bay (36° 34′ N, 6° 16′ W, a station influenced by the Guadalete River). Transects were performed by sailing from the Outer Bay to the Inner Bay logging *in situ* surface fluorescence, temperature and

salinity data each second at a mean speed of 6 knots with a SeaBird25 CTD. We also used this instrument to obtain vertical profiles of temperature, salinity and depth for each day and station. Samples were taken using a 6L-Niskin bottle. At the Inner Bay, because of it is shallow depth, water was collected only at the surface, whereas for the Outer Bay and the Strait of Puntales the samples were collected at surface and at depth (ca. 9.2 m for the Outer Bay and 6.5 m for the Strait of Puntales) (Table 1). Samples were collected from 7:30 and 11:38 UTC hours and during ebb tides except for June. The tidal conditions were neap tides for the sampling dates of March, May, and September, intermediate tide on July 1st and spring tides for June and late July.

Samples were filtered using precombusted (550 °C, 1 h) Whatman GF/F glass fiber filters (0.7 μm nominal pore-size). The filtrate for determining CDOM optical properties was immediately stored at 4 °C in the dark. For the analysis of dissolved organic carbon (DOC), 50 μl of orthophosphoric acid 25% was added to aliquots of the filtered water in 20 ml pre-combusted amber vials, and the samples were stored at 4 °C in the dark until analysis. To determine bacterial abundance, we filled 5-ml vials with unfiltered water and 0.5 ml of glutaraldehyde at 50% and stored them at −80 °C.

2.3. Measurements

CDOM absorbance was performed using a spectrophotometer (Perkin Elmer Lambda 40, connected to a computer equipped with UVWinlab software). All samples were measured in duplicate with 10 cm pathlength quartz cuvettes, previously rinsed with Milli-Q water. Prior to spectral acquisition, the instrument was calibrated and a Milli-Q water blank was run to reference all sample spectra. Spectra were scanned over the wavelength range of 200–800 nm. The average absorbance value within the range 700–800 nm was subtracted from each absorbance scan to correct for scattering. To minimize temperature effects all samples were equilibrated to room temperature prior to measurement. Absorbance at a wavelength of 355 nm was expressed as a Naperian absorption coefficient (a_{355}) and calculated by multiplying the absorbance value (A) by 2.303 and dividing by the cuvette pathlength (l) in meters:

$$a_{\mathrm{CDOM}} = \frac{2.303 \cdot (A - A_{700-800})}{l}$$

The molar absorption coefficients (ε) ($m^2\ mol^{-1}$) were calculated by dividing each absorption coefficient by DOC concentration (C) in millimoles.

$$\varepsilon_{\mathrm{CDOM}} = \frac{a_{\mathrm{CDOM}}}{C}$$

The spectral slopes $S_{275-295}$ and $S_{350-400}$ were obtained from the regression line of the Naperian logarithms of the absorption coefficients vs. wavelengths. These ranges, 275–295 nm and 350–400 nm, were chosen because the higher variability in the slope (S) occurs in these two intervals, especially between 275 and 295, which confers a high sensitivity of this parameter to DOM character changes (Helms et al., 2008). The S_R ratio was calculated by dividing $S_{275-295}$ by $S_{350-400}$, and its changes appear to be related to variations in the DOM molecular weight (Helms et al., 2008).

Two of the fluorescence techniques utilized by biogeochemical oceanographers include the "peak picking" determination (Coble, 1996) and the fluorescence index (FI) calculation (McKnight et al., 2001). We scanned samples for fluorescence in a 1 cm pathlength quartz cuvette, previously rinsed several times with Milli-Q water. The EEMs were measured with a JY-Horiba Spex Fluoromax-4 spectrophotometer and were scanned using an integration time of 0.25 s over an excitation range of 240–450 nm at 10 nm increments and over an emission range of 300–560 nm at 2 nm increments. Spectral acquisition was performed in "signal-to-reference" (S:R) mode and instrument-specific excitation and emission corrections were applied. All samples were normalized to the Raman area to account for lamp decay over time and inner-filter correction was also applied. Milli-Q blanks were subtracted to eliminate the Raman peak. The EEMs generation and corrections were carried out using MATLAB 7.6.0 (R2008a). For each water sample, the fluorescence peaks were measured at the maximum fluorescence intensity (reported in Raman units (R.U.) at an excitation–emission wavelength pair). We identified the five peaks proposed by Coble (1996, 2007): two terrestrial humic-like peaks (A and C) and one marine humic-like peak (M) that excite within the range 240–360 and fluoresce within the range 370–460 nm and two amino acid-like peaks (B and T) that excite at 275 and 280 nm and fluoresce at 310 and 340, respectively. The FI was obtained from corrected EEMs as the ratio of intensities emitted at 470 and 520 nm at an excitation of 370 nm (Cory and McKnight, 2005).

DOC concentration was measured as non-purgeable organic carbon on samples acidified to pH 2 with orthophosphoric acid 25% using a Shimadzu TOC-V_{CPH}. The chlorophyll a concentration ($\mu g\ L^{-1}$) was fluorometrically determined by extraction with 90% acetone (Joint Global Ocean Flux Study Protocols, 1994). Bacterial abundance was determined by flow cytometry. The samples for bacterial abundance were thawed, shaken and stained using Sybr green II (1:10,000 dilution of Molecular Probes commercial solution) for 3 min in the dark and run through a flow cytometer (Coulter Epics Elite) at low flow rate (50 $\mu l\ min^{-1}$). Bacteria were discriminated by their green fluorescence. A stock solution of yellow–green 0.98 μm latex beads (Molecular Probes) was added as an internal standard.

Statistical analysis of the correlations and the slopes comparisons (t-tests) were performed using Statistica 7.0. The Student's t-test (t), the degrees of freedom (df) and the p-value were reported for the slope comparisons.

3. Results

3.1. DOC concentration and CDOM absorbance

DOC concentrations ranged from 83 to 477 μM (Table 1). The maximum values were observed during the dry season: at the Strait of Puntales during September at depth, at the Outer Bay also in September but in surface samples with a peak concentration of 228 μM, and at the Inner Bay in July with a peak concentration of 243 μM.

Absorption coefficients at 355 nm ranged from 0.30 m^{-1} to 1.99 m^{-1} (Table 1). In general, these values were higher during the dry season than during the rainy season (Fig. 2). Like DOC concentrations, the maximum value of the absorption coefficients was observed at the Strait of Puntales at depth during September. In fact, we found a significant and positive relationship between DOC concentration and the a_{355} values ($n = 27$, $r = 0.73$, $p < 0.001$).

Molar absorption coefficients at 355 nm (i.e. the absorption per carbon unit) ranged from 3.5 to 10.3 $m^2\ mol^{-1}$ in the Strait of Puntales; from 2.3 to 6.8 $m^2\ mol^{-1}$ in the Inner Bay; and from 2.7 to 6.4 $m^2\ mol^{-1}$ in the Outer Bay (Table 1). The ε_{355} values were generally higher in surface than in deep waters, particularly in the Strait of Puntales and during the rainy season.

In terms of the S_R, a surrogate of the relative molecular weight of the DOM pool, the values ranged from 0.85 to 2.05. The lowest S_R value (i.e. the highest mean molecular weights) was found in the deep waters at the Strait of Puntales during the dry season (Table 1).

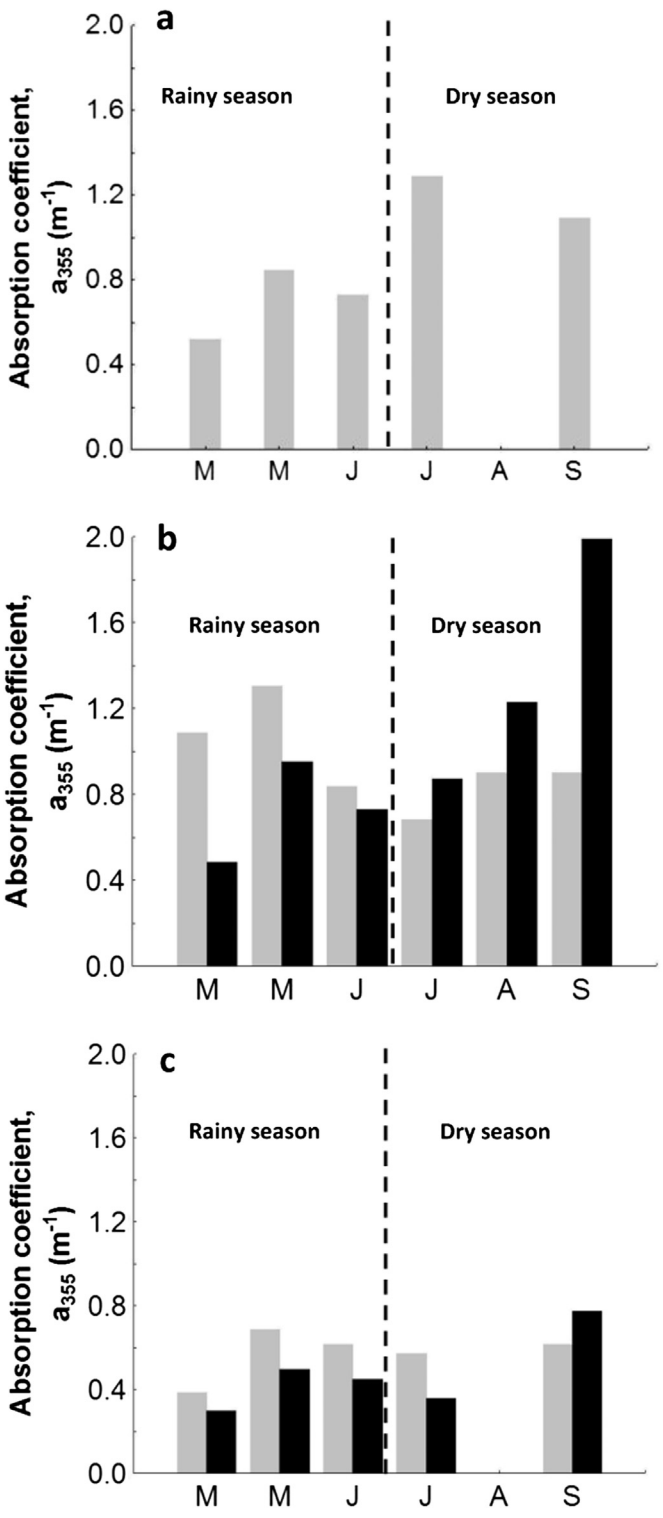

Fig. 2. Values of the absorption coefficients at 355 nm (a_{355}) in surface (gray bars) and in deep (black bars) waters at the three study stations: (a) Inner Bay, (b) Strait of Puntales, and (c) Outer Bay. A dashed line separates the rainy vs. dry period. The August bar corresponds to the sampling date of July 26th.

3.2. CDOM fluorescence

The values of the fluorescence index (FI) ranged from 1.48 to 1.62 (Table 1). Using the nomenclature of Coble (1996), we identified two terrestrial humic-like peaks: peak A (Ex/Em 240/440 nm) and peak C (Ex/Em 350/440 nm) and one marine humic-like peak M (Ex/Em 310/420 nm); and the two amino acid-like peaks: peak T (Ex/Em 240(300)/340) and peak B (Ex/Em 270/300), which are similar in fluorescence to tryptophan and tyrosine amino acids (Fig. 3). The humic-like riverine influence on FDOM is evident by comparing the peak A of the EEM from the Guadalete River (Fig. 3a) with the EEM of the Strait of Puntales in surface waters (Fig. 3b), but this peak is less relevant in samples collected at depth (Fig. 3c).

The fluorescence intensity of peak T went up substantially from below detection level up to 12.01 R.U. with the maximum values at the Strait of Puntales in samples collected at depth during the dry season (Fig. 4). The fluorescence intensity of peak B ranged from 0.01 to 3.94 R.U. Likewise, the peak B fluorescence also showed the highest values at the Strait of Puntales in samples collected at depth during the dry season (Fig. 4). In contrast, at the Outer Bay the maximum values of both peaks were coincident with the chlorophyll *a* peaks in May and September (Table 1), but we did not obtain any statistically significant relationship (see below).

In relation to the humic-like peaks, the fluorescence intensity of peak A ranged from 0.05 to 0.45 R.U. This peak showed the highest values at the Strait of Puntales during the dry period at depth, being particularly high in September, and during the rainstorms of March (Fig. 5). The Inner Bay also showed high fluorescence intensities of peak A with its maximum in July (Fig. 5). The fluorescence intensity of peak C ranged from 0.02 to 0.09 R.U. and showed a seasonal pattern similar to peak A (Fig. 5). The fluorescence intensity of peak M ranged from 0.02 to 1.29 R.U. with the highest fluorescence intensities during the dry season at depth in the Strait of Puntales (Fig. 5). Overall, it was during the dry season, particularly in the deep waters of the Strait of Puntales, when all the fluorophores (peaks A, C, M, T and B) increased drastically (Figs. 4 and 5, note the large-scale changes).

3.3. CDOM and FDOM drivers

We observed a significant correlation between the water level of the Guadalete river and the ε_{355} ($n = 27$, $r = 0.46$, $p < 0.05$; Fig. 6a), with the highest values recorded at the Strait of Puntales station (black dots, Fig. 6a) and the lowest values at the Outer Bay (white dots, Fig. 6a). Similarly, the relative fluorescence of peak A (a fluorophore representative of humic-like component of terrestrial origin) with respect to DOC concentration was also significantly correlated to the water level of the Guadalete river ($n = 27$, $r = 0.43$, $p < 0.05$; Fig. 6b), with the highest values also at the Puntales Strait station and the lowest ones at the Outer Bay (white dots, Fig. 6b).

The values of chlorophyll *a* ranged from 0.83 μg l^{-1}–7.72 μg l^{-1}, with maximum peaks at the end of March and beginning of May in all the stations (Table 1). However, we did not find significant relationships between chlorophyll *a* and the absorbance-derived parameters (i.e. a_{355}, ε_{355}, and S_R) or the fluorescence intensities of peaks A, C, M, B or T. Bacterial abundance ranged from 0.37×10^6 cell ml^{-1} and 3.52×10^6 cell ml^{-1} with the maximum values measured in the Inner Bay in September (Table 1). As with chlorophyll *a*, we did not find any significant relationships between bacterial abundance and the absorbance or fluorescence parameters determined in this study.

Salinity values ranged from 34.96 to 37.40 psu reaching values above 36 psu during the dry season and higher values in the Inner Bay than in the Outer Bay (Table 1). We found positive and significant correlations between salinity and DOC concentration (Fig. 7a), absorption coefficients (Fig. 7b) and all the fluorescence peaks (Fig. 7c, d and e). The slope of the DOC vs. salinity correlation was 49 (±20) and for a_{355} vs. salinity was 0.26 (±0.09). The slope of the linear regression for salinity vs. the terrestrial humic-like peak A was 0.06 (±0.02) and for salinity vs. peak C was 0.01 (±0.00)

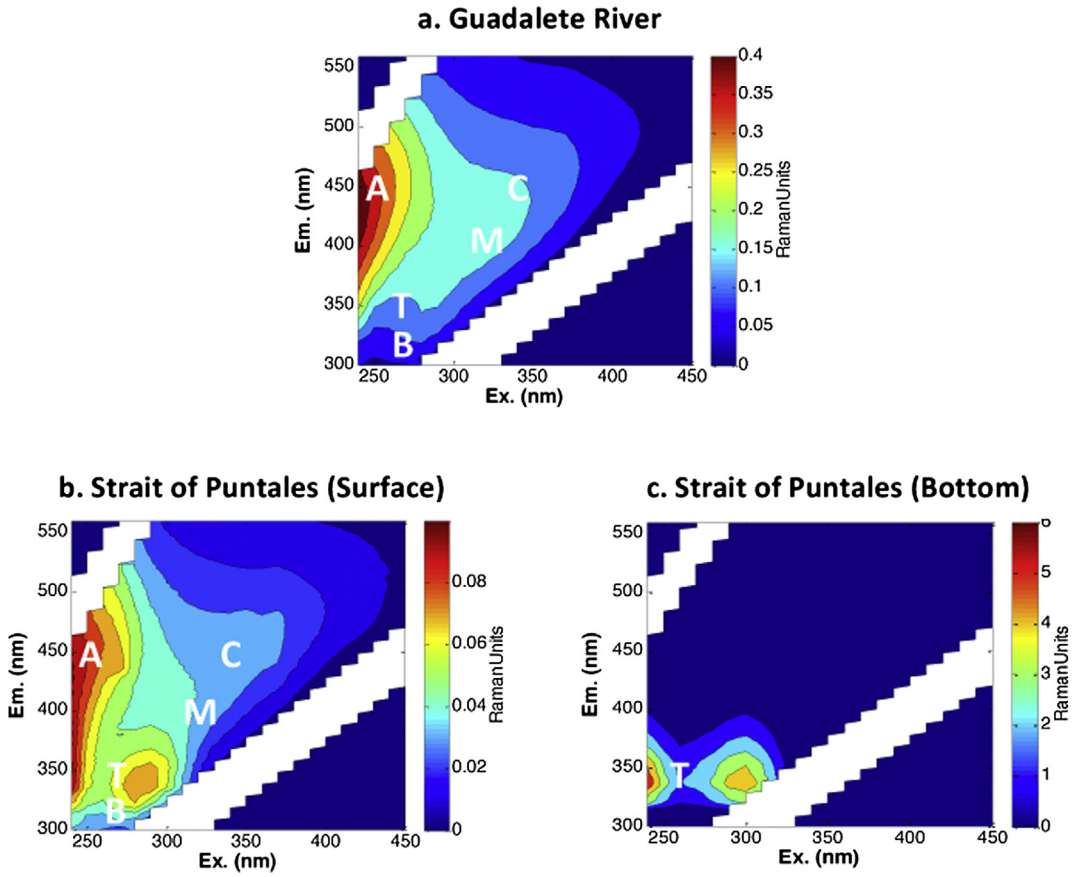

Fig. 3. Representative three-dimensional excitation emission matrixes (EEMs) of fluorescent dissolved organic matter of the end-member Guadalete River (a) and in surface (b) and bottom (c) waters at Strait of Puntales during July. Note the scale for the EEMs in surface and deep water is substantially different.

(Fig. 7c). The difference between these two slopes was significant ($t = 2.50$, df = 23, $p < 0.05$), and both were lower than the slope of salinity vs. a_{355} ($t = 2.90$, df = 23, $p < 0.01$ and $t = 2.81$, df = 23, $p < 0.01$, respectively). The slope between salinity and the marine humic-like peak M was 0.25 (±0.09), similar to the a_{355} slope ($p > 0.05$). The slopes between salinity and the amino acid-like components were 0.62 (±0.18) for peak T and 0.41 (±0.14) for peak B. These last slopes were significantly higher than the slope for a_{355} ($t = 3.96$, df = 23, $p < 0.001$ and $t = 2.94$, df = 23, $p < 0.01$, respectively).

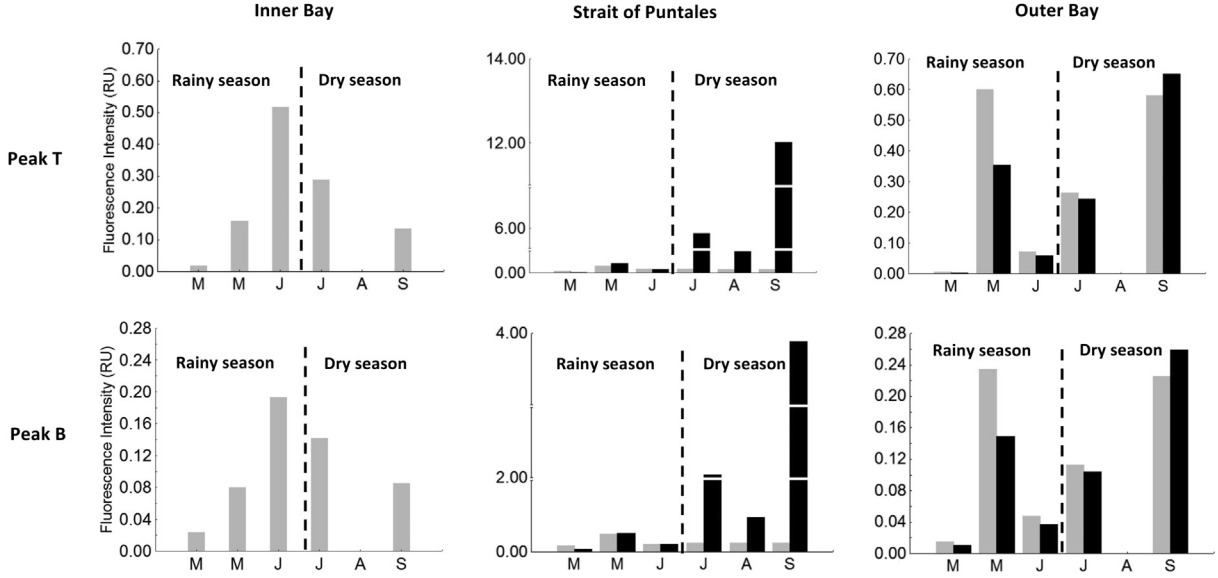

Fig. 4. Fluorescence intensity of the amino acid-like components (peak T and peak B) at the Inner Bay, Strait of Puntales, and Outer Bay. A dashed line separates the rainy vs. dry period. The August bar corresponds to the sampling date of July 26th. Note the scale for the Strait of Puntales is different and discontinuous.

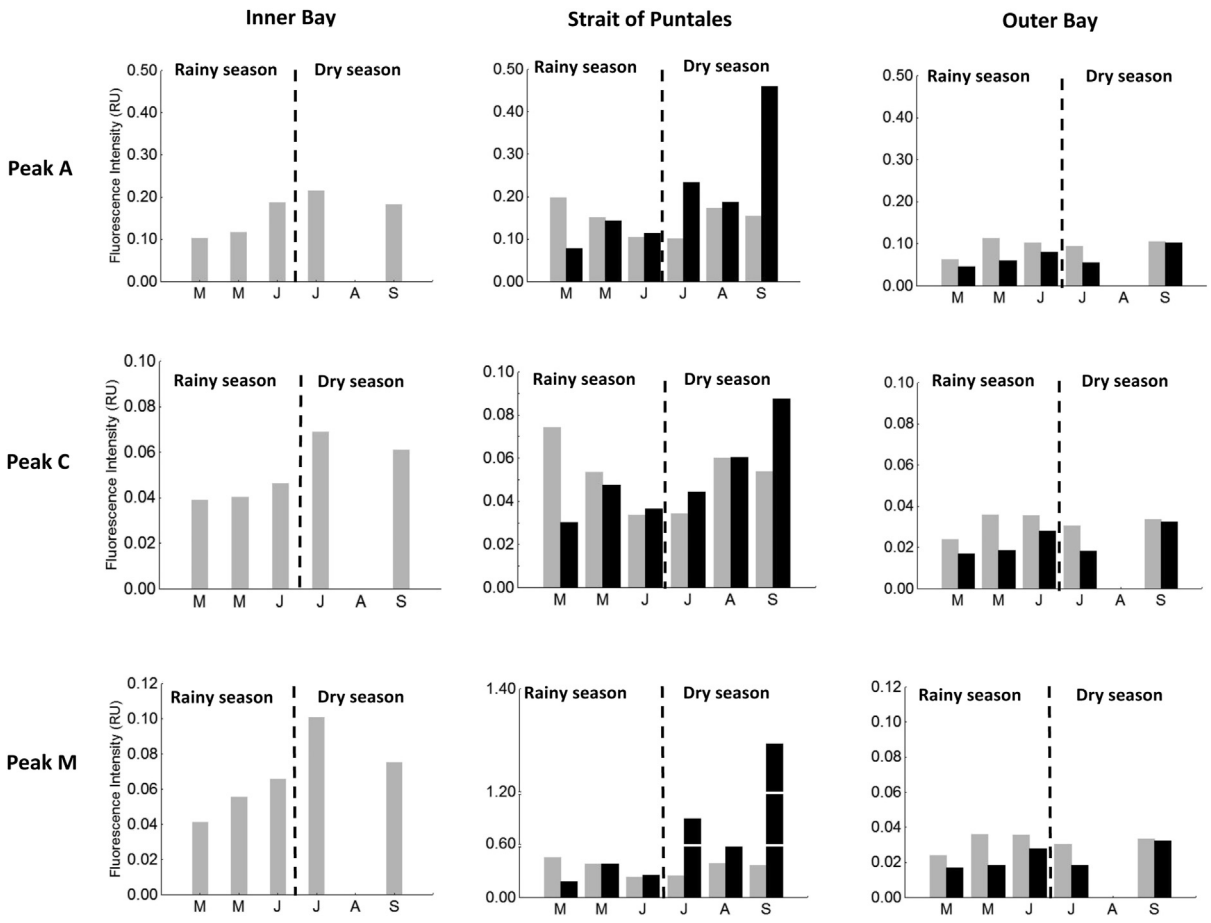

Fig. 5. Fluorescence intensity of the terrestrial (peak A and peak C) and marine (peak M) humic-like components at the Inner Bay, Strait of Puntales, and Outer Bay. A dashed line separates the rainy vs. dry period. The August bar corresponds to the sampling date of July 26th. Note the scale for the intensity of peak M is different and discontinuous at the Strait of Puntales.

4. Discussion

4.1. CDOM sources and sinks during rainy and dry periods

DOC concentrations, a_{355} values, and the spectral slopes obtained in the study system were similar to the values found in other coastal systems, such as the Po River estuary (Berto et al., 2010), Chesapeake Bay (Rochelle-Newall and Fisher, 2002; Helms et al., 2008) and Florida Bay (Stabenau et al., 2004). The range of FI values in this study reflect contributions of both microbial and terrestrial inputs (McKnight et al., 2001) and appear to reflect a higher influence of autochthonous production than the comparatively lower values found by Singh et al. (2010) in the Barataria Basin, another marshland-rich estuary.

During rainy periods, the DOM pool is expected to contain a higher proportion of chromophoric, humic-like components derived from riverine discharge (e.g. Del Castillo et al., 1999; Granskog et al., 2007). Indeed, the water level of Guadalete river (Fig. 1) was significantly correlated with the relative content of chromophores (molar absorption) and terrestrial humic-like fluorophore A normalized by DOC concentration (Fig. 6). This is consistent with the notion that the riverine input contributes terrestrial DOM from the mainland to the estuary, irrespective of relationships between the water level and freshwater discharges during the rainy period or tidal inflow/outflows.

During the dry season, in the absence of rainfall and relevant riverine discharge, alternative CDOM sources have been reported. In Southern California, Clark et al. (2008) showed increasing CDOM exports from salt marshes toward coastal waters during ebb tides. They also showed that the different plants found in salt marshes produced terrestrial humic-like components (peaks A and C), but especially marine humic-like (peak M) and amino acid-like (peak T) components. Similarly, Milbrandt et al. (2010) found higher FDOM values during ebb tides, and in particular the peak M increased up to eight-fold. In our study system, all sampling was performed during ebb tides except the June sampling. In fact, we also observed more than an order of magnitude increase in the intensity of peak M during this season (Fig. 5). In addition, given that the timing of spring tides occurs in summer, we might expect the highest outputs from the salt marshes during this period. Effectively, the Inner Bay presented the highest absolute values of a_{355} and humic-like fluorescence at this time (Figs. 2 and 5), which did not correspond to stream runoff. At the Puntales Strait Station, the absorption coefficients (Fig. 2) as well as the fluorescence of peaks M, T and B were more than one order of magnitude higher during the dry than the rainy season (Figs. 4 and 5), especially in the deep waters collected just above the sediments (Fig. 3c).

These high CDOM values in deep waters may reflect diffusion from pore water sediments upwards and/or CDOM drain-out at depth from the salt marshes of the Inner Bay towards the Outer Bay, as is the typical circulation pattern of inverse estuaries. Moreover, Clark et al. (2008) found that all CDOM exported from salt marshes cannot be attributed only to fresh leachates from marsh plants, and that it may also be partially released from marsh sediments. In addition, Burdige et al. (2004) reported that refractory, humic-like compounds are preferentially preserved in sediments compared to

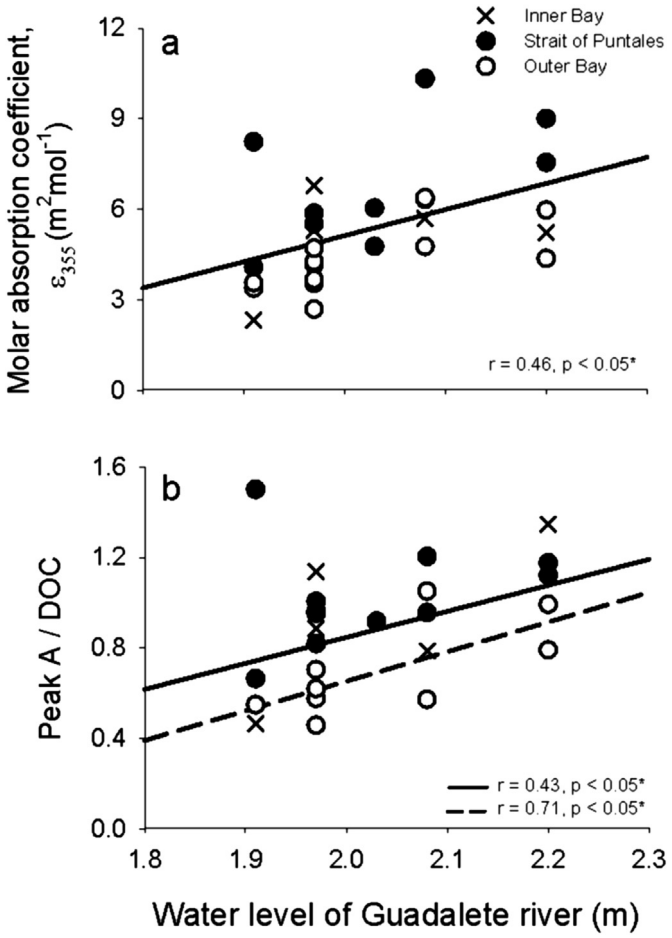

Fig. 6. Relationships between water level in the Guadalete River and (a) the molar absorption coefficients at 355 nm, ε_{355}, and (b) the peak A normalized by the DOC concentration. Dashed regression line indicates the relationship between the water level in the Guadalete River and the peak A/DOC ratio exclusively at the Outer Bay.

the amino acid-like compounds that appear to be transported out of the sediments by diffusion. Therefore, the extremely high fluorescence values of the amino acid-like peak T and B at the Strait of Puntales at depth may reflect *in situ* production of FDOM from coastal and salt marsh sediments.

Another alternative CDOM source can be the DOC released by seagrasses (Barrón and Duarte, 2009). Stabenau et al. (2004) reported that submerged seagrass beds might contribute to CDOM with an apparent terrestrial/humic signature either directly during their senescence or indirectly through bacterial processing of the labile DOM released by seagrass. In fact, Brun et al. (2003) have reported vast extensions of seagrass in the Bay of Cádiz, although no direct measurements of its contribution to CDOM pool have been performed.

On the other hand, sewage pollution may also contribute to the increase the fluorescence intensity of peak B (Baker and Spencer, 2004). In our study system, Morris et al. (2009) reported a spectacular increase of sewage inputs associated with an intensification of tourism during the summer. Therefore, sewage inputs are another likely source of amino acid-like components into the Bay that should be considered in future studies.

Photobleaching, the major CDOM sink, is the loss of absorbance due to solar radiation (Mopper et al., 1991). In coastal waters, the net photobleaching effects may be masked due to continuous riverine CDOM inputs, strong vertical mixing and tides (Del Vecchio and Blough, 2002). This situation appears to occur in the Bay of Cádiz, especially during the rainy season, since CDOM and the intensities of peaks A and C were higher in surface waters than at depth.

During the dry season, DOM photobleaching is expected to be more intense, especially in shallow bays where most of the water column is sunlight exposed. In fact, in the Strait of Puntales we observed lower CDOM values (Fig. 2) and fluorescence intensities of peaks A, C and M (Fig. 5) in surface waters than at depth. In previous studies (Nelson et al., 1998; Nieto-Cid et al., 2006; Ortega-Retuerta et al., 2010b), this depletion of surface CDOM has been attributed to photobleaching losses. Also, in Arctic surface waters, humic-like fluorophores A and C have been found to be more photo-labile than protein-like components (Stedmon and Markager, 2005; Laurion and Mladenov, 2013), and may be preferentially photodegraded in estuarine surface waters as well.

4.2. CDOM trends along salinity gradients

Salinity is considered to be a good tracer for the mixing between fresh- and marine waters in estuarine and coastal systems and, therefore, reflects the potential significance of riverine inputs enriched in terrestrial humic-like components. In temperate and tropical estuaries with regular rainy periods and continuous runoff inputs, negative relationships between salinity and absorption coefficients (Del Castillo et al., 1999; Jaffé et al., 2004; Kowalczuk et al., 2005; Osburn and Stedmon, 2011) and particularly between salinity and terrestrial humic-like fluorophores are prevalent (Yamashita et al., 2008, 2011). In contrast, the Mediterranean climate is characterized by an annual precipitation that hardly exceeds 900 mm and with rainfall mostly restricted to fall and spring. This peculiarity results in very variable water levels in Mediterranean rivers and, consequently, runoff inputs in estuarine and coastal areas are very low and unpredictable. During the dry season, the negative hydrological budget generated by intense evaporation (Corlis et al., 2003) produces hypersaline conditions and, consequently, inverse circulation patterns (Largier et al., 1997).

Unlike other studies in temperate and tropical estuaries (e.g. Kowalczuk et al., 2006; Yamashita et al., 2008; Guo et al., 2011), the absorption coefficients and the fluorescence intensities of peaks A, C, M, B and T in water of the Bay of Cádiz did not show conservative mixing (i.e. negative trends with salinity). By contrast, DOC concentration, absorption coefficients and the fluorescence intensities of all humic- and amino acid-like peaks increased with salinity (Fig. 7).

Several reasons might explain these positive trends, but with different slopes, between salinity and absorption coefficients and the fluorescence peaks. The simplest explanation for these positive trends is the inverse nature of Cádiz Bay during the dry season. In these conditions, hypersaline water of the Inner Bay, which is enriched in CDOM from the salt marshes, becomes diluted as it circulates towards the ocean at ebb tides. This oceanic dilution of hypersaline waters is responsible for positive salinity-CDOM trend. If this mixing is conservative and dilution is the main driver, our slopes should be similar to those reported in the literature for estuaries with conservative mixing, but with the opposite sign. In fact, the slope of the relationship between a_{355} and salinity (0.26) was in the same range (−0.1 to −0.65) as those reported by other authors that observed conservative mixing in temperate and tropical systems (Del Castillo et al., 1999; Kowalczuk et al., 2006; Osburn and Stedmon, 2011).

The slopes for relationships between salinity and each fluorescence peak, however, varied widely from +0.01 to +0.62. Assuming that the a_{355} slope is a gross average for most chromophoric

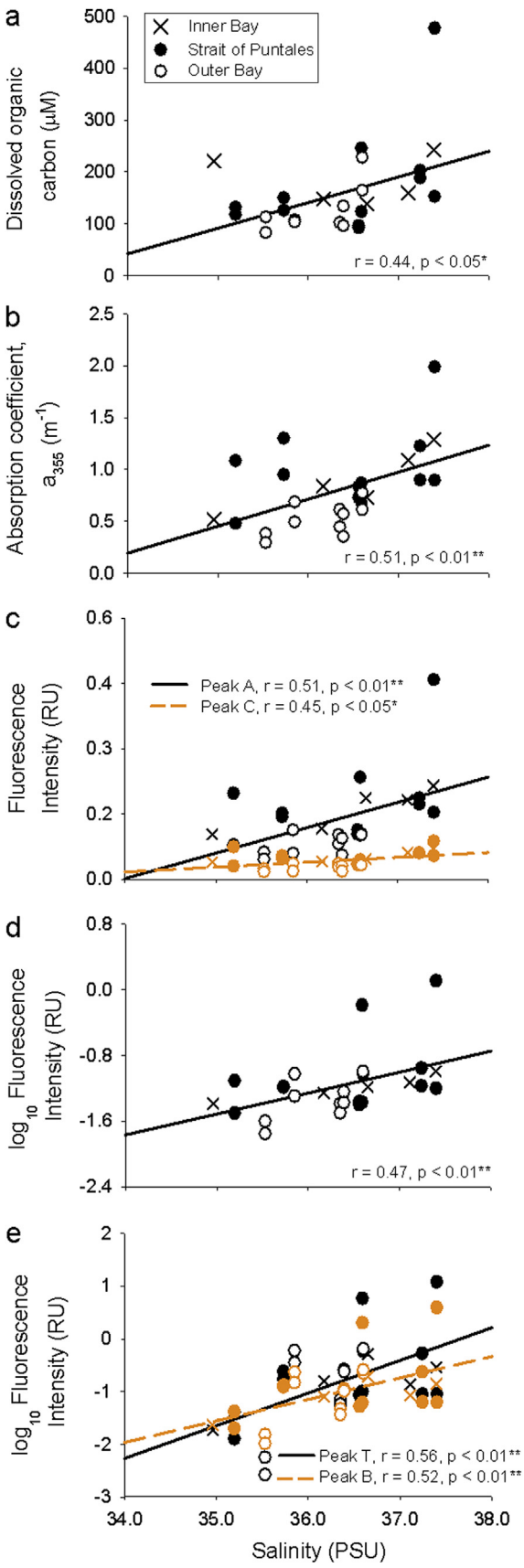

Fig. 7. Correlations between salinity and the dissolved organic carbon concentration (DOC) (a), the absorption coefficients at 355 nm (a_{355}) (b), the fluorescence intensity of Peak A (black, solid line) and peak C (orange, dashed line) (c), the fluorescence intensity of Peak M (d), and the fluorescence intensity of Peak T (black, solid line) and B (orange, dashed line) (e). Fluorescence intensity of peaks M, T and B were log10 transformed to fit normality. (For interpretation of the references to color in this figure legend, the reader is referred to the web version of this article.)

components, the two terrestrial humic-like peaks (A and C) presented significantly lower slopes than the a_{355} slope suggesting a preferential loss of these fluorophores during the dilution process towards the ocean. An important sink of these fluorophores could be photobleaching. In fact, photobleaching of humic components has been already reported in the literature (Skoog et al., 1996; Nieto-Cid et al., 2006). In addition, Osburn and Stedmon (2011) also obtained a very low slope (−0.003) for the humic-like component (C3-peak A) in the Baltic sea, similar to the slope obtained in this study for the peak A (+0.006), but of different sign. By contrast, the slopes for the two amino acid-like fluorophores were significantly higher than the a_{355} slope suggesting an *in situ* production of these components during its mixing with the oceanic waters. The sources of these amino acid-like components may be attributed to direct diffusion from salt marsh or coastal sediments (Burdige et al., 2004; Clark et al., 2008) or to microbial production (Coble, 1996; Yamashita and Tanoue, 2003; Yamashita et al., 2008). Also, the less photo-labile nature of amino acid-like components (compared to humic-like components) and their preservation during greater solar exposure may contribute to the relationships observed between peaks B and T and salinity.

On the other hand, the hypersaline conditions impose a higher ionic strength than the oceanic waters and it is known that DOM optical properties are ionic-sensitive (Reche et al., 1999; Dryer et al., 2008). In fact, Pace et al. (2012) demonstrated that increases in alkaline conditions produced shifts in DOM conformation that increase its absorption capacity and photobleaching rates. Boyd and Osburn (2004) also observed changes in CDOM spectral properties associated with a salinity gradient that may be attributed to conformational changes with potential implications for DOM biodegradability. Therefore, salinity itself, by directly promoting conformational changes or indirectly with more photodegraded DOM also being more biodegradable and able to boost microbial activity, may increase marine humic-like or amino acid-like fluorophores. However, we did not find relationships between the absorption coefficients or fluorescence peaks and bacterial abundance. Therefore, the link to microbial activity is more tenuous.

In summary, the inverse nature of the Bay of Cádiz during the dry season could be responsible for the observed positive trends between CDOM/FDOM and salinity. The underlying mechanism likely is the simple dilution of hypersaline, CDOM enriched water of the Inner Bay by the less saline, more oceanic water of the Outer Bay. The lower slopes of the humic-like components (peaks A and C) in comparison with the a_{355} slope suggest preferential losses of A and C fluorophores during the mixing with the oceanic water. These losses likely are related to photobleaching. By contrast, the higher slopes of the amino acid-like components (peaks B and T) in comparison with the a_{355} slope suggest an *in situ* production of these fluorophores or more photo-refractory nature of these components. These increases likely are related to the diffusion from salt marsh and coastal sediments and their microbial DOM processing.

Acknowledgments

We appreciate very much the constructive revision by Dr. D.G. Bowers that improved a previous version of this work. We would like to thank to the participants in the Bahía Project (PO6-RNM-01637) for providing us the logistic to carry out our study. Specially, we thank Reyes Sánchez and Natalia Garzón for their willingness to

help us and facilitate all the Bahía Proyect data. Besides, we thank Óscar Sánchez Romero and Gabriel Navarro for the support with Matlab 7.6.0. (R2008a) software and E. P. Morris for supplying background information about Cadiz Bay generated within the project FUNDIV (PO7-RNM-02516) and for providing us with useful information of the Guadalete river flow. We thank to the anonymous reviewers for their suggestions to improve the previous version of this manuscript.

References

Álvarez, O., Izquierdo, A., Tejedor, B., Mañanes, R., Tejedor, L., Kagan, B.A., 1999. The influence of sediment load on tidal dynamics, a case study: Cádiz Bay. Estuar. Coast. Shelf Sci. 48, 439–450.

Baker, A., Spencer, R.G.M., 2004. Characterization of dissolved organic matter from source to sea using fluorescence and absorbance spectroscopy. Sci. Total. Environ. 333, 217–232.

Barrón, C., Duarte, C., 2009. Dissolved organic matter release in a *Posidonia oceanica* meadow. Mar. Ecol. Prog. Ser. 374, 75–84.

Berto, D., Giani, M., Savelli, F., Centanni, E., Ferrari, C.R., Pavoni, B., 2010. Winter to spring variations of chromophoric dissolved organic matter in a temperate estuary (Po River, Northern Adriatic Sea). Mar. Environ. Res. 70 (1), 73–81.

Bianchi, T.S., Wysocki, L.A., Schreiner, K.M., Filley, T.R., Corbett, D.R., Kolker, A.S., 2010. Sources of terrestrial organic carbon in the Mississippi plume region: evidence for the importance of coastal marsh inputs. Aquat. Geochem. 17 (4–5), 431–456.

Bowers, D.G., Evans, D., Thomas, D.N., Ellis, K., Williams, P.J.L.B., 2004. Interpreting the colour of an estuary. Estuar. Coast. Shelf Sci. 59 (1), 13–20.

Bowers, D.G., Brett, H.L., 2008. The relationship between CDOM and salinity in estuaries: an analytical and graphical solution. J. Marine Syst. 73 (1–2), 1–7.

Boyd, T.J., Osburn, C.L., 2004. Changes in CDOM fluorescence from allochthonous and autochthonous sources during tidal mixing and bacterial degradation in two coastal estuaries. Mar. Chem. 89, 189–210.

Brun, F.G., Pérez-Llorérns, J.L., Hernández, I., Vergara, J.J., 2003. Patch distribution and within-patch dynamics of the Seagrass Zostera noltii Hornem. in Los Toruños Salt-Marsh, Cádiz Bay, Natural Park. Spain. Bot. Mar. 46 (6), 513–524.

Burdige, D.J., Kline, S.W., Chen, W., 2004. Fluorescent dissolved organic matter in marine sediment pore waters. Mar. Chem. 89 (1–4), 289–311.

Clark, C.D., Litz, L.P., Grant, S.B., 2008. Salt marshes as a source of chromophoric dissolved organic matter (CDOM) to Southern California coastal waters. Limnol. Oceanogr. 53 (5), 1923–1933.

Coble, P.G., 1996. Characterization of marine and terrestrial DOM in seawater using excitation-emission matrix spectroscopy. Mar. Chem. 51, 325–346.

Coble, P.G., del Castillo, C.E., Avril, B., 1998. Distribution and optical properties of CDOM in the Arabian Sea during the 1995 southwest Monsoon. Deep-Sea Res. II 45, 2195–2223.

Coble, P.G., 2007. Marine optical biogeochemistry: the chemistry of ocean color. Chem. Rev. 107, 402–418.

Corlis, N.J., Herbert Veeh, H., Dighton, J.C., Herczeg, A.L., 2003. Mixing and evaporation processes in an inverse estuary inferred from δ^2H and $\delta^{18}O$. Cont. Shelf Res. 23 (8), 835–846.

Cory, R.M., McKnight, D.M., 2005. Fluorescence spectroscopy reveals ubiquitous presence of oxidized and reduced quinones in dissolved organic matter. Environ. Sci. Technol. 39 (21), 8142–8149.

De la Paz, M., Gómez-Parra, A., Forja, J., 2008. Variability of the partial pressure of CO_2 on a daily-to-seasonal time scale in a shallow coastal system affected by intensive aquaculture activities (Bay of Cádiz, SW Iberian Peninsula). Mar. Chem. 110, 195–204.

Del Castillo, C.E., Coble, P.G., Morell, J.M., López, J.M., Corredor, J.E., 1999. Analysis of the optical properties of the Orinoco river plume by absorption and fluorescence spectroscopy. Mar. Chem. 66, 35–51.

Del Vecchio, R., Blough, N.V., 2002. Photobleaching of chromophoric dissolved organic matter in natural waters: kinetics and modeling. Mar. Chem. 78 (4), 231–253.

Dryer, D.J., Korshin, G.V., Fabbricino, M., 2008. In situ examination of the protonation behavior of fulvic acids using differential absorbance spectroscopy. Environ. Sci. Technol. 42 (17), 6644–6649.

Fellman, J.B., D'Amore, D.V., Hood, E., Boone, R.D., 2008. Fluorescence characteristics and biodegradability of dissolved organic matter in forest and wetland soils from coastal temperate watersheds in southeast Alaska. Biogeochemistry 88 (2), 169–184.

Fellman, J.B., Petrone, K.C., Grierson, P.F., 2011. Source, biogeochemical cycling, and fluorescence characteristics of dissolved organic matter in an agro-urban estuary. Limnol. Oceanogr. 56 (1), 243–256.

Ferrón, S., Ortega, T., Forja, J.M., 2009. Benthic fluxes in a tidal salt marsh creek affected by fish farm activities: Río San Pedro (Bay of Cádiz, SW Spain). Mar. Chem. 113, 50–62.

Gardner, G.B., Chen, R.F., Berry, A., 2005. High resolution measurements of chromophoric dissolved organic matter (CDOM) in the Neponset River Estuary, Boston Harbor, MA. Mar. Chem. 96, 137–154.

González-Gordillo, J.I., Rodríguez, A., 2003. Comparative seasonal and spatial distribution of decapod larvae assemblages in three coastal zones off the southwestern Iberian Peninsula. Acta Oecol. 24, 219–233.

Granskog, M.A., Macdonald, R.W., Mundy, C.J., Barber, D.G., 2007. Distribution, characteristics and potential impacts of chromophoric dissolved organic matter (CDOM) in Hudson Strait and Hudson Bay, Canada. Cont. Shelf Res. 27 (15), 2032–2050.

Guo, W., Stedmon, C.A., Han, Y., Wu, F., Yu, X., Hu, M., 2007. The conservative and non-conservative behavior of chromophoric dissolved organic matter in Chinese estuarine waters. Mar. Chem. 107 (3), 357–366.

Guo, W., Yang, L., Hong, H., Stedmon, C.A., Wang, F., Xu, J., Xie, Y., 2011. Assessing the dynamics of chromophoric dissolved organic matter in a subtropical estuary using parallel factor analysis. Mar. Chem. 124, 125–133.

Helms, J.R., Stubbins, A., Ritchie, J.D., Minor, E.C., Kieber, D.J., Mopper, K., 2008. Absorption spectral slopes and slope ratios as indicators of molecular weight, source, and photobleaching of chromophoric dissolved organic matter. Limnol. Oceanogr. 53 (3), 955–969.

Jaffé, R., Boyer, J.N., Lu, X., Maie, N., Yang, C., Scully, N.M., Mock, S., 2004. Source characterization of dissolved organic matter in a subtropical mangrove-dominated estuary by fluorescence analysis. Mar. Chem. 84, 195–210.

Joint Global Ocean Flux Study, 1994. Protocols for the Join Global Ocean Flux Study Core Measurements. Intergovernmental Oceanographic Commission, SCOR, pp. 91–96. Manual and Guides, Unesco 29.

Kowalczuk, P., Ston-Egiert, J., Cooper, W.J., Whitehead, R.F., Durako, M.J., 2005. Characterization of Chromophoric Dissolved Organic Matter (CDOM) in the Baltic Sea by Excitation Emission Matrix Fluorescence Spectroscopy.

Kowalczuk, P., Stedmon, C.A., Markager, S., 2006. Modeling absorption by CDOM in the Baltic Sea from season, salinity and chlorophyll. Mar. Chem. 101 (1–2), 1–11.

Lalli, C.M., Parsons, T.R., 1997. Biological Oceanography: an Introduction. Butterworth-Heinemann Ltd, Oxford England, p. 314.

Largier, J.L., Hollibaugh, J.T., Smith, S.V., 1997. Seasonally hypersaline estuaries in Mediterranean-climate regions. Estuar. Coast. Shelf Sci. 45, 789–797.

Laurion, I., Mladenov, N., 2013. Dissolved organic matter photolysis in Canadian arctic thaw ponds. Environ. Res. Lett. 8 (3), 035026.

Maie, N., Yamashita, Y., Cory, R.M., Boyer, J.N., Jaffé, R., 2012. Application of excitation emission matrix fluorescence monitoring in the assessment of spatial and seasonal drivers of dissolved organic matter composition: sources and physical disturbance controls. Appl. Geochem. 27 (4), 917–929.

McKnight, D.M., Boyer, E.W., Westerhoff, P.K., Doran, P.T., Kulbe, T., Andersen, D.T., 2001. Spectrofluorometric characterization of dissolved organic matter for indication of precursor organic material and aromaticity. Limnol. Oceanogr. 46, 38–48.

Milbrandt, E.C., Coble, P.G., Conmy, R.N., Martignette, A.J., Siwicke, J.J., 2010. Evidence for the production of marine fluorescence dissolved organic matter in coastal environments and a possible mechanism for formation and dispersion. Limnol. Oceanogr. 55, 2037–2051.

Mopper, K., Zhou, X., Kieber, R.J., Kieber, D.J., Sikorski, R.J., Jones, R.D., 1991. Photochemical degradation of dissolved organic carbon and its impact on the oceanic carbon cycle. Nature (London) 353, 60–62.

Morris, E.P., Peralta, G., Benavente, J., Freitas, R., Rodríguez, A.M., Quintino, V., Alvarez, O., Valcárcel-Pérez, N., Vergara, J.J., Hernández, I., Pérez-Lloréns, J.L., 2009. Caulerpa prolifera stable isotope ratios reveal anthropogenic nutrients within a tidal lagoon. Mar. Ecol. Prog. Ser. 390, 117–128.

Nelson, N.B., Siegel, D.A., Michaels, A.F., 1998. Seasonal dynamics of coloured dissolved material in the Sargasso Sea. Deep-Sea Res. I 45, 931–957.

Nelson, N.B., Carlson, C.A., Steinberg, D.K., 2004. Production of chromophoric dissolved organic matter by Sargasso Sea microbes. Mar. Chem. 89, 273–287.

Nelson, N.B., Siegel, D.A., 2013. The global distribution and dynamics of chromophoric dissolved organic matter. Ann. Rev. Marine Sci. 5, 447–476.

Nieto-Cid, M., Álvarez-Salgado, X.A., Pérez, F.F., 2006. Microbial and photochemical reactivity of fluorescent dissolved organic matter in a coastal upwelling system. Limnol. Oceanogr. 50 (3), 1391–1400.

Nunes-Vaz, R.A., 2012. The salinity response of an inverse estuary to climate change & desalination. Estuar. Coast. Shelf Sci. 98 (C), 49–59.

Opsahl, S., Benner, R., 1997. Distribution and cycling of terrigenous dissolved organic matter in the ocean. Nature 386, 480–482.

Ortega-Retuerta, E., Frazer, T.K., Duarte, C.M., Ruiz-Halpern, S., Tovar-Sanchez, A., Arrieta, J.M., Reche, I., 2009. Biogeneration of chromophoric dissolved organic matter by bacteria and krill in the Southern Ocean. Limnol. Oceanogr. 54 (6), 1941–1950.

Ortega-Retuerta, E., Siegel, D.A., Nelson, N.B., Duarte, C.M., Reche, I., 2010a. Observations of chromophoric dissolved and detrital organic matter distribution using remote sensing in the Southern Ocean: validation, dynamics and regulation. J. Marine Syst. 82, 295–303.

Ortega-Retuerta, E., Reche, I., Pulido-Villena, E., Agustí, S., Duarte, C.M., 2010b. Distribution and photoreactivity of chromophoric dissolved organic matter in the Antarctic Peninsula (Southern Ocean). Mar. Chem. 118, 129–139.

Osburn, C.L., Stedmon, C.A., 2011. Linking the chemical and the optical properties of dissolved organic matter in the Baltic-North Sea transition zone to differentiate three allocthonous inputs. Mar. Chem. 126, 281–294.

Pace, M.L., Reche, I., Cole, J.J., Ferna, A., Mazuecos, I.P., Prairie, Y.T., 2012. pH change induces shifts in the size and light absorption of dissolved organic matter. Biogeochemistry 108, 109–118.

Reche, I., Pace, M.L., Cole, J.J., 1999. Relationship of trophic and chemical conditions to photobleaching of dissolved organic matter in lake ecosystems. Biogeochemistry 44, 259–280.

Rochelle-Newall, E.J., Fisher, T.R., 2002. Chromophoric dissolved organic matter and dissolved organic carbon in Chesapeake Bay. Mar. Chem. 77, 23–41.

Romera-Castillo, C., Sarmento, H., Álvarez-Salgado, X.A., Gasol, J.M., Marrasé, C., 2010. Production of chromophoric dissolved organic matter by marine phytoplankton. Limnol. Oceanogr. 55 (1), 446–454.
Romera-Castillo, C., Sarmento, H., Alvarez-Salgado, X.A., Gasol, J.M., Marrase, C., 2011. Net production and consumption of fluorescent colored dissolved organic matter by natural bacterial assemblages growing on marine phytoplankton exudates. Appl. Environ. Microbiol. 77, 7490–7498.
Siegel, D.A., Maritorena, S., Nelson, N.B., Behrenfeld, M.J., McClain, C.R., 2005. Colored dissolved organic matter and its influence on the satellite-based characterization of the ocean biosphere. Geophys. Res. Lett. 32 (20).
Singh, S., D`Sa, E.J., Swenson, E.M., 2010. Chromophoric dissolved organic matter (CDOM) variability in Barataria Basin using excitation-emission matrix (EEM) fluorescence and parallel factor analysis (PARAFAC). Sci. Total. Environ. 408, 3211–3222.
Skoog, A., Wedborg, M., Fovelqvist, E., 1996. Photobleaching of fluorescence and the organic carbon concentration in a coastal environment. Mar. Chem. 55, 333–345.
Stabenau, E., Zepp, R., Bartels, E., Zika, R., 2004. Role of the seagrass Thalassia testudinum as a source of chromophoric dissolved organic matter in coastal south Florida. Mar. Ecol. Prog. Ser. 282, 59–72.
Stedmon, C.A., Markager, S., Bro, R., 2003. Tracing dissolved organic matter in aquatic environments using a new approach to fluorescence spectroscopy. Mar. Chem. 82, 239–254.
Stedmon, C.A., Markager, S., 2005. Resolving the variability in dissolved organic matter fluorescence in a temperate estuary and its catchment using PARAFAC analysis. Limnol. Oceanogr. 50 (2), 686–697.
Steinberg, D.K., Nelson, N.B., Carlson, C.A., Prusak, A.C., 2004. Production of chromophoric dissolved organic matter (CDOM) in the open ocean by zooplankton and the colonial cyanobacterium Trichodesmium *spp*. Mar. Ecol. Prog. Ser. 267, 45–56.
Tremblay, L.B., Dittmar, T., Marshall, A.G., Cooper, W.J., Cooper, W.T., 2007. Molecular characterization of dissolved organic matter in a North Brazilian mangrove porewater and mangrove-fringed estuaries by ultrahigh resolution Fourier transform-ion cyclotron resonance mass spectrometry and excitation/emission spectroscopy. Mar. Chem. 105 (1–2), 15–29.
Tzortziou, M., Neale, P.J., Osburn, C.L., Megonigal, J.P., Maie, N., Jaffé, R., 2008. Tidal marshes as a source of optically and chemically distinctive colored dissolved organic matter in the Chesapeake Bay. Limnol. Oceanogr. 53, 148–159.
Yamashita, Y., Tanoue, E., 2003. Chemical characterization of protein-like fluorophores in DOM in relation to aromatic amino acids. Mar. Chem. 82, 255–271.
Yamashita, Y., Jaffé, R., Maie, N., Tanoue, E., 2008. Assessing the dynamics of dissolved organic matter (DOM) in coastal environments by EEM-PARAFAC. Limnol. Oceanogr. 53, 1900–1908.
Yamashita, Y., Panton, A., Mahaffey, C., Jaffé, R., 2011. Assessing the spatial and temporal variability of dissolved organic matter in Liverpool Bay using excitation–emission matrix fluorescence and parallel factor analysis. Ocean Dynam. 61, 569–579.